



Plasma Induced Line Shifts and Their Effects on Line Merging and Population Kinetics

**D.A. Haynes, Jr., G.C. Junkel,
M.A. Gunderson, C.F. Hooper, Jr.**

March 2000

UWFDM-1125

Presented at the Twelfth APS Topical Conference on Atomic Processes in Plasmas, Reno NV, 19-23 March 2000.

FUSION TECHNOLOGY INSTITUTE

UNIVERSITY OF WISCONSIN

MADISON WISCONSIN

DISCLAIMER

This report was prepared as an account of work sponsored by an agency of the United States Government. Neither the United States Government, nor any agency thereof, nor any of their employees, makes any warranty, express or implied, or assumes any legal liability or responsibility for the accuracy, completeness, or usefulness of any information, apparatus, product, or process disclosed, or represents that its use would not infringe privately owned rights. Reference herein to any specific commercial product, process, or service by trade name, trademark, manufacturer, or otherwise, does not necessarily constitute or imply its endorsement, recommendation, or favoring by the United States Government or any agency thereof. The views and opinions of authors expressed herein do not necessarily state or reflect those of the United States Government or any agency thereof.

**Plasma Induced Line Shifts and Their Effects on Line
Merging and Population Kinetics**

D. A. Haynes, Jr.

Fusion Technology Institute
Department of Engineering Physics
University of Wisconsin-Madison
1500 Engineering Drive
Madison, WI 53706

G. C. Junkel, M. A. Gunderson, and C. F. Hooper, Jr.

Department of Physics
University of Florida
Gainesville, Florida 32611

March 2000

UWFDM-1125

Abstract

Plasma-induced line shifts to the red have been observed in a number of laser-produced plasmas. After briefly reviewing some of the more recent of these observations and a method of calculating their magnitude, two implications of the existence of these shifts are explored. Firstly, calculations show for plasma conditions such as those in the reviewed experiments the red shifts are larger for lines originating from manifolds with higher principal quantum numbers. This leads to line merging at lower densities than would be expected without considering shifts. Secondly, even though the observed shifts are small with respect to kT_e they can have a substantial effect on population kinetics calculations for loosely bound states which approximate the effects of continuum lowering on level populations through the use of effective statistical weights.

Recent Experimental Observations of Plasma Induced Line Shifts: A Brief Review

Over the past several years a number of experimental observations and measurements of plasma induced line shifts have been reported.^{1,2,3,4,5} This section briefly reviews the results from these studies, providing the motivation for our consideration of the implications of these shifts.

Leng, Goldhar, Griem, and Lee report the observation of C VI Lyman line profiles emitted by a plasma produced by the interaction of a 100 mJ 10-ps KrF laser pulse with a graphite target.¹ The plasma thus produced had densities $\lesssim 10^{22} \text{ cm}^{-3}$ and electron temperatures $\lesssim 200$ eV. The time-integrated spectrograph had a resolution of better than 50 mÅ in the spectral range containing the C VI Lyman- α , - β , and - γ lines. Their analysis included the effects of spatial integration along the line of sight using a multi-layer model of the plasma. The Lyman- γ line is clearly observed to shift to the red. Their multi-layer model, including the effects of Stark broadening, plasma-induced line shifts, and Doppler broadening provides a substantially better fit to the observed Lyman- γ line than did a model which did not include the effect of shifts (see Figure 4 of Reference 1). The calculation used for plasma induced line shifts in their model was that of Nguyen, et al.⁶

In an experiment explicitly designed to observe plasma produced line shifts, Renner, et al.² measured the location of the Lyman- α through - η lines at various locations (corresponding to different densities) in a quasi-one dimensional columnar Al plasma. This column of plasma was produced by irradiating an Al microdot evaporated onto a plastic substrate with 170 J of 0.44 μm radiation in a 400 ps pulse. The plastic constrained the Al plasma into a columnar flow with small transverse velocities. The correspondence between location in the column and electron density relied on radiative hydrodynamic modeling of the system, but was checked by comparing the measured width of the Al Lyman- γ line as a function of position along the column with Stark broadened line profiles calculated for the densities predicted by the computer simulation. They observed an approximately linear increase in the magnitude of the red shift as a function of ion density, and that shift varied approximately as the fourth power of the principal quantum number of the upper level of the transition. Though the observed shifts were only 8 – 10% of the line widths, they were significantly larger than any experimental uncertainties.

In a series of directly-driven microballoon implosions conducted using the Omega laser system at the Laboratory for Laser Energetics, Hooper, et al.³ observed time-resolved K-shell spectra from the Ar-doped deuterium fuel. In these experiments, 20 μm thick plastic microballoons of approximately 0.9 mm outer radius were filled with 20 atm of deuterium doped with 0.125% Ar (atomic percentage). These microballoons were imploded by the 60 beam Omega laser delivering approximately 28 kJ to the target in a 1 ns square pulse. During the resulting implosion, the core gas reached electron densities above 10^{24} cm^{-3} and electron temperatures of 1.5 keV, as inferred by fitting the Ar K-shell spectrum to a theoretical model including the Ar He and Ly- α , - β , and - γ lines and associated satellites. The spectrum from the times around stagnation were well fit using a single density and temperature, confirming radiative hydrodynamic simulations which predict small gradients of these quantities in the most emissive part of the core. In Figure 1 we display a series of time-resolved Ar K-shell spectra recorded during such an implosion. The dispersion relation was determined at early times (low densities). Because the time resolution was accomplished

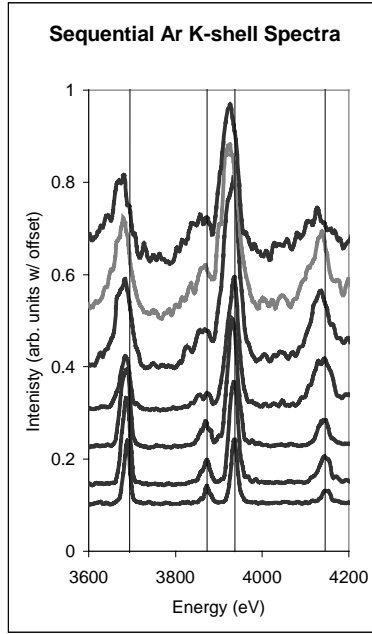


FIGURE 1. A sequence of Ar K-shell spectra recorded in 30 ps intervals during the implosion of a microballoon filled with Ar-doped deuterium. The vertical lines are at the isolated ion locations of (from left to right) the Ar He- β , - γ , Ly- β and - γ lines. The sequential spectra are shifted vertically by arbitrary amounts for presentation, with the lowest spectra being earliest.

using an x-ray streak camera, known streak camera distortions⁷ (curvature of isotime lines, and streak angle) had to be taken into account. In Figure 1, one sees that as time progresses and the density increases, the lines get broader (due to Stark broadening) and shift to the red, with the γ lines shifting more than the β lines. Indeed, the composite spectral feature formed by the Ar He- γ and Ly- β lines serves as an excellent test bed for shift studies,

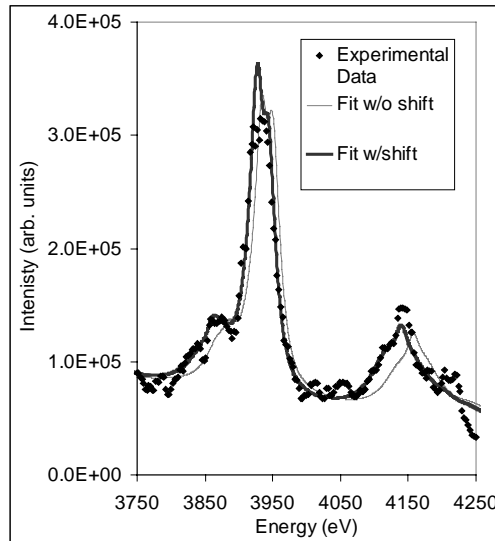


FIGURE 2. Detail from the penultimate spectrum in Figure 1, along with results from theoretical calculations for Ar K-shell emission from a uniform plasma of electron density 10^{24} cm^{-3} and temperature of 1.4 keV. The two fits shown differ in whether or not the effects of plasma induced line shifts were included in the calculation.

as their proximity reduces possible errors which might be introduced due to experimental uncertainties, and as their relative shift is a strong function of density for these plasma conditions.

A fit of the model spectrum to the spectral region including the Ar He- γ , Ly- β and - γ from second lineout from the top of Figure 1 is shown in Figure 2, for calculations when the model spectrum did and did not include the effects of plasma produced line shifts.

The final work noted in this brief review of experimental observations of plasma induced line shifts is that of Woolsey, et al.⁵ In this series of indirectly driven implosion experiments performed using the Nova laser system at Lawrence Livermore National Laboratory stable, reproducible high energy density Ar-doped deuterium plasmas were produced. A high-resolution ($\lambda/\Delta\lambda \sim 1800$) crystal spectrometer coupled to an x-ray streak camera recorded emission from the Ar He- β lines and its associated Li-like satellites with 30 ps time resolution. In essence, they inferred the density from the width of the He- β line and the temperature from the relative intensity of the resonance line and the Li-like satellites. By measuring the shift of the composite spectral feature, the shift as a function of density of the He- β line was determined. For an electron density of $6.2 \times 10^{23} \text{ cm}^{-3}$ and temperature of 800 eV, they report a red shift of $4 \text{ m}\text{\AA} \pm 2 \text{ m}\text{\AA}$, and show that the variation of shift as a function of density is approximately linear.

In these five examples of recent observations of plasma induced line shifts, the line positions are found to shift to the red approximately linearly with increasing electron density. Given this accumulation of evidence for the existence of plasma induced line shifts, it is appropriate to consider the implications of these shifts. Following a brief review of one method of calculating the shifts, the implications of these shifts on line merging and population kinetics will be explored.

Calculation of Stark Broadened Line Shapes Including the Effects of Plasma Induced Line Shifts

For charged radiators, plasma induced line shifts arise naturally out of Stark broadening theory calculations which do not make the dipole approximation to $V_{e,r}$, the interaction between the radiator electrons and the plasma electrons. For multi-electron charged radiators immersed in hot plasmas two full Coulomb theories of line broadening have been implemented at the University of Florida: a quantum mechanical theory⁸ which retains all terms to second order in $V_{e,r}$, and an all-order semiclassical theory⁹. Here we will concentrate on the quantum mechanical calculation, though a comparison of the results from the two methods will be shown for plasma conditions relevant to the experiments discussed in Reference 3.

We begin with an expression¹⁰ for the lineshape function, $I(\omega)$:

$$I(\omega) = \frac{4\omega^4}{3c^3} \int d\vec{E} Q(\vec{E}) J(\omega; \vec{E})$$

where $Q(\vec{E})$ is the ion microfield probability distribution function, here calculated using the APEX¹¹ method. $J(\omega; \vec{E})$ is the electron broadened and shifted line profile emitted by a radiator experiencing a plasma ion microfield, \vec{E} . Our line shape calculations include the effects of ion dynamics^{12,13} (required because of the low mass of the deuterium perturbers and the high temperature in the core of the microballoon implosions). $J(\omega; \vec{E})$ is given by

$$J(\omega; \vec{E}) = -\frac{1}{\pi} \text{Re Tr}_r \left[\vec{d} \cdot R(\omega; \vec{E}) \rho_r \vec{d} \right].$$

In the BID¹² formulation for ion dynamics effects, the resolvent $R(\omega; \vec{E})$ is

$$R(\omega; \vec{E}) = \frac{G(\Delta\omega; \vec{E})}{1 + i\nu(\Delta\omega) \int d\vec{E}' Q(\vec{E}') G(\Delta\omega; \vec{E}')},$$

and, finally, $G(\omega; \vec{E})$ is related to the familiar resolvent for the static ion approximation with an additional broadening term due to the effect of the motion of the ions,

$$G(\Delta\omega; \vec{E}) = \frac{1}{\Delta\omega - L_{i,r}(\vec{E}) - B - M(\Delta\omega) - i\nu(\Delta\omega)}.$$

Here, $\Delta\omega$ is the separation from the unperturbed location of the transition, $L_{i,r}$ is the Liouville operator associated with the interaction of the radiator with the plasma ion microfield, $\nu(\Delta\omega)$ is a measure of the effects of perturber ion motion on the radiator. We are primarily concerned with the terms associated with the interaction of the radiator with the plasma electrons, B and $M(\Delta\omega)$. Though we separate the frequency independent B from the rest of the electron-radiator interaction term, we stress that this does not stem from the ad hoc addition of a shift term to the formalism. This frequency independent shift arises organically from the theory so long as the dipole approximation to the radiator-electron interaction term is not made.

The appropriateness of truncating the calculation at terms second order in $V_{e,r}$ has been explored by Cooper, Kelleher, and Lee.¹⁴ They offer a criterion of minimum temperature,

$$kT > \frac{Z(Z-1)}{n^2} (\text{Ry})$$

which the experimental results discussed here satisfy with the exception the observation of the Al Ly- α by Saemann, et al. in Reference 4. For charged radiators when this criterion is met the dominant contribution to the line shift is from the first term in the expansion of B in powers of $V_{e,r}$, $B^{(1)}$:

$$B^{(1)} = n_e \text{Tr}_1 \left[L_1(r, 1) f_0(1) \right],$$

where n_e is the plasma electron density, the trace is over the coordinates of a single perturbing electron, the Liouville operator is that associated with the interaction of the plasma electron with the radiator electrons, and $f_0(1)$ is the distribution function for a plasma electron in the field of the ion. This term is explicitly linear in electron density. Results are given in Figure 3 for the shift for the first three members of the Ar He Rydberg series using the quantum mechanical second order theory and are compared with the published results of Reference 6 and Griem, et al.¹⁵

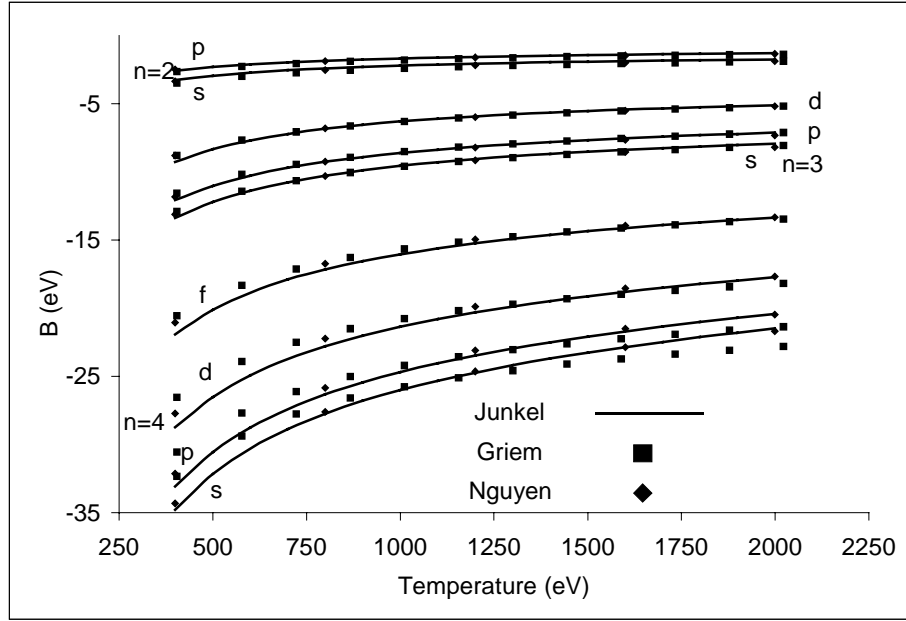


FIGURE 3. Comparison of shifts calculated for the Ar He-like transitions arising from $n=2$, 3, and 4, for an electron density of 10^{24} cm^{-3} for various temperatures using the theories of References 8 (Junkel), 15 (Griem) and 6 (Nguyen).

In Figure 3 two salient features of plasma induced shifts are indicated. The plasma-induced shift is a strong function of the principal quantum number of the upper state of the transition, and emission from states with differing angular quantum numbers shift differently. The dependence on angular quantum number can be thought of as arising from the dependence of the expectation value of the radius of an atomic orbital on that quantum number. This dependence leads to predictions of marked asymmetries of γ lines at the temperatures and densities found in the core of microballoon implosions such as those in References 3 and 5. In Figure 4 the effect of the shift is illustrated in calculations of the first three members of the Ar Ly series.

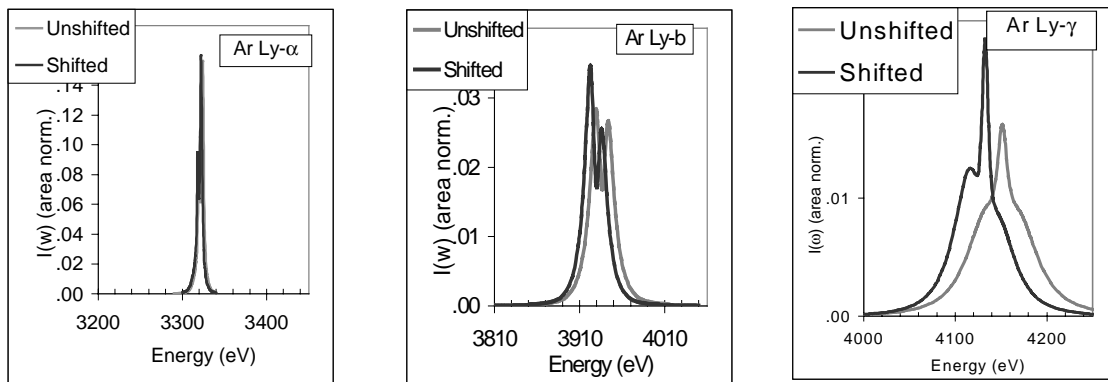


FIGURE 4. Stark broadened lineshapes for the Ar Ly- α , - β , and - γ lines, calculated for an electron density of 10^{24} cm^{-3} and an electron temperature of 1 keV. The results of two calculations are presented for each transition, “Shifted” (including B in the resolvent) and “Unshifted” (artificially setting B to zero in the calculation).

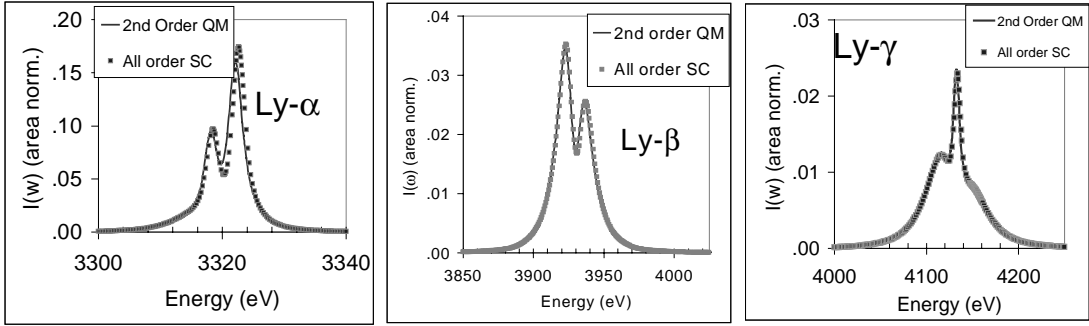


FIGURE 5. Stark broadened lineshapes for the Ar Ly- α , - β , and - γ lines, calculated for an electron density of 10^{24} cm^{-3} and an electron temperature of 1 keV, calculated using an all order semiclassical formalism (All order SC), and a quantum mechanical formalism which retains terms to 2nd order in $V_{e,r}$ (2nd Order QM).

The importance of effects of terms of $O[V_{e,r}^3]$ and higher can be estimated by comparing the results of the second order quantum mechanical theory to the all-order semi-classical theory. For plasma conditions relevant to the stagnated core of microballoon implosion experiments the effect of these higher order terms is small for the first three lines in the Ar Ly Rydberg series, as is illustrated in Figure 5.

Implications of the Existence of Plasma Induced Line Shifts on Line Merging and Population Kinetics Calculations

Having reviewed recent experimental observations and measurements of plasma induced line shifts and outlined their calculation, we now turn to a consideration of the implications of the existence of plasma induced line shifts on line merging and population kinetics calculations.

Recall the observations of Renner, et al.²: shifts that approximately scaled linearly with density and the fourth power of principal quantum number. Extrapolating these observations to higher densities, one would expect that for each sequential pair in a Rydberg series there exists a density at which the lines are emitted at the same frequency, and above which the lines reverse order. Clearly, this is an inappropriate extrapolation. Indeed, there are off-diagonal terms in the spherically symmetric B_l which mix states from different principal quantum numbers which have the same ℓm . What occurs is that the states from the coalescing manifolds mix so that it is no longer appropriate to speak of separate lines; instead a composite is formed which continues to shift to the red. Before that point is reached, when the lines are distinct, they do have a separation that is smaller than their isolated atom value. Thus, estimates of density from the Inglis-Teller limit¹⁶ should account for plasma induced line shifts in order to arrive at a more accurate bound on density. The effects of line merging are illustrated in Figure 6.

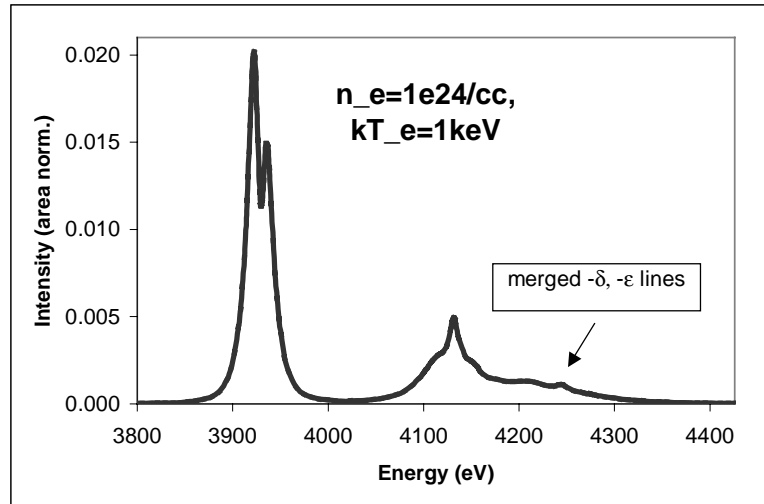


FIGURE 6. Simultaneous calculation of the Ar Ly- β , - γ , - δ , and - ϵ lines, including the effects of line merging for an electron density of 10^{24} cm^{-3} and an electron temperature of 1 keV, calculated using a quantum mechanical formalism which retains terms to 2nd order in $V_{e,r}$ (2nd Order QM).

Perhaps a more subtle implication of the existence of plasma induced line shifts occurs when the effects of level shifts of the same order of magnitude on population kinetics calculations are considered. Because such shifts are small with respect to kT , one might assume that generally they could have only negligible effects on population distributions. However, when the effects of continuum lowering are considered, kT is not the only energy scale to consider. When continuum lowering is important, the ionization energy for a level becomes relevant. For some lines, the shift can be a significant fraction of the ionization energy. Here, as an example, we consider the effects of level shifts, equal to the observed line shifts, on the degeneracy lowering formalism of Hummer and Mihalas.

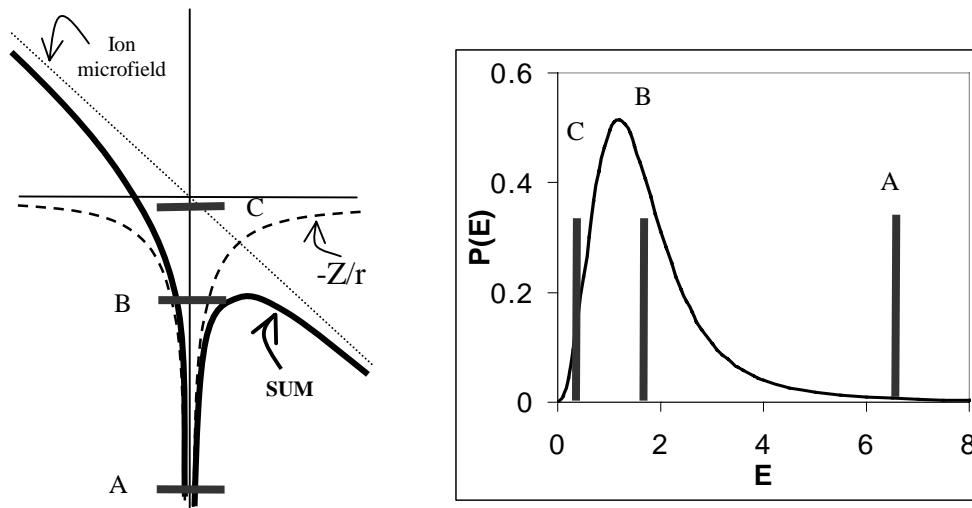


FIGURE 7. Left: sketch of the potentials associated with the interaction of a radiator electron with the nucleus and the ion microfield, their sum, and the location of three bound states. Right: ion microfield probability distribution function with the values needed to field ionize the marked states indicated.

In Figure 7, the quasi-static potentials affecting a radiator immersed in a plasma are sketched. For a given value of the ion microfield, the shape of the sum of the Coulomb interaction with the nucleus and the ion microfield can be thought of as defining three broad classes of states that are bound for the isolated atom. States such as A are tightly bound and are not much affected by the microfield. States that are loosely bound in the isolated ion, such as C, are field ionized. States, like B, near the threshold can either be effectively ionized or bound, depending on whether their energy matches resonance conditions in the effective potential. On the right side of Figure 7, a typical form for the ion microfield probability distribution for a given temperature and density is sketched, and the field values needed to ionize states A, B, and C are indicated. For a plasma at that temperature and density, few radiators experience fields sufficient to ionize state A, while most experience ion microfields sufficient to ionize state C. Roughly half of the radiators experience ion microfields sufficient to ionize state B. Hummer and Mihalas¹⁷ suggest that the fraction of ions for which a given state remains bound be used to modify the effective statistical weight of that state in population kinetics calculations:

$$g(\Delta\chi_1; n_e, kT) = g_0 \left[1 - \int_{E(\Delta\chi_1)}^{\infty} dE P(E; n_e, kT) \right].$$

In this expression, $g(\Delta\chi_1; n_e, kT)$ is the effective statistical weight of a state with ionization potential $\Delta\chi_1$ in a plasma with electron density and temperature n_e, kT respectively. It is equal to the product of the isolated ion statistical weight of the state, g_0 , and the fraction of ions in the plasma for which the state remains bound. This fraction is given by the integral of the ion microfield probability distribution function, $P(E; n_e, kT)$ from 0 to the field classically required to ionize the state, $E(\Delta\chi_1)$. The resulting $g(\Delta\chi_1; n_e, kT)$ varies smoothly with temperature and density, avoiding the unphysical effects of suddenly removing states from the kinetics model. However, $g(\Delta\chi_1; n_e, kT)$ varies rapidly as a function of $\Delta\chi_1$ for values corresponding to those near the peak of $P(E; n_e, kT)$, as is illustrated in Figure 8.

In Figure 8 $\left[1 - \int_{E(\Delta\chi_1)}^{\infty} dE P(E; n_e, kT) \right]$, the degeneracy modification parameter is plotted

for an Ar radiator immersed in a deuterium plasma (1% Ar doping) of electron densities of $1 \times 10^{24} \text{ cm}^{-3}$ and $2 \times 10^{24} \text{ cm}^{-3}$ and an electron temperature of 1 keV as a function of $\Delta\chi_1$. Also indicated are the isolated atom location of the upper level of the Ar Ly- γ line and locations of the upper level shifted by the amount calculated for the line shift using the 2nd order quantum mechanical formalism. A naïve implementation of plasma-induced line shifts into a CRE population kinetics calculation would modify the degeneracy lowering parameter of the $n=4$ $^3P_{1/2}$ level by 12% and 33% for plasma with electron densities of $1 \times 10^{24} \text{ cm}^{-3}$ and $2 \times 10^{24} \text{ cm}^{-3}$, respectively, with even larger increases for less tightly bound levels.

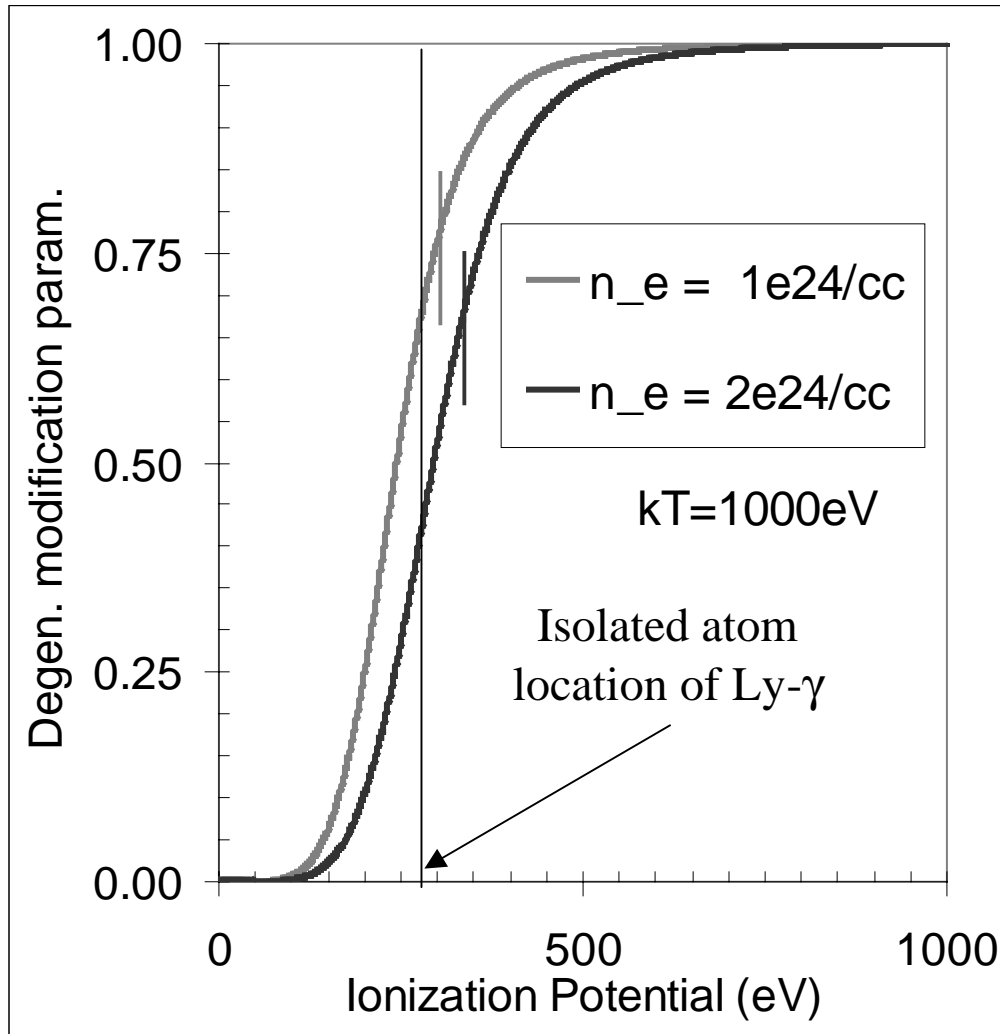


FIGURE 8. The degeneracy modification parameter as a function of ionization potential for Ar radiators immersed in a deuterium plasma (1% Ar doping) and an electron density of $1 \times 10^{24} \text{ cm}^{-3}$ and $2 \times 10^{24} \text{ cm}^{-3}$ and an electron temperature of 1 keV. Indicated are the isolated ion location of the Ar Ly- γ , and the amount by which the line shifts for each density.

Conclusion

Plasma induced line shifts have been observed and measured in a variety of hot dense plasmas.^{1,2,3,4,5} For plasmas with temperatures sufficiently high to justify the use of a truncated expansion of the plasma electron-radiator there exist at least four methods of calculating these shifts, all of which reasonably agree for the plasma conditions in Figure 3.^{6,8,9,15} The existence of these shifts has led us to consider their implications on line merging and population kinetics. Because lines originating from manifolds with higher values of the principal quantum number, n , shift more than do those from manifolds with lower n , line merging effects such as those considered by Ingliss and Teller¹⁶ occur at lower densities than would be the case if there were no shifts. If, for time scales relevant to population kinetics calculations, the levels associated with the observed lines can be treated as having shifted by an amount equal to the observed line shift, then the effects of the shift on the effective degeneracy should be taken into account, even though the shifts are small with respect to kT_e .

Acknowledgement

Funding for the work was provided by the U.S. Department of Energy National Laser Facility User Program.

References

-
- ¹ Y. Leng, J. Goldhar, H. R. Griem, and R. W. Lee, *Phys. Rev. E* **52**, 4238 (1995).
- ² O. Renner, P. Sondhaus, D. Salzmann, A. Djaoui, M. Koenig, and E. Förster, *J. Quant. Spectrosc. Radiat. Transfer* **58**, 851 (1997).
- ³ C. F. Hooper, Jr., G. Junkel, M. Gunderson, D. A. Haynes, Jr., R. C. Mancini, D. K. Bradley, J. A. Delettrez, and P. Jaanimagi, in “Strongly Coupled Coulomb Systems”, eds. G. Kalman, J. M. Rommel, and K. Blagoev, p. 385 (Plenum 1998).
- ⁴ A. Saemann, K. Eidmann, I. E. Golovkin, R. C. Mancini, E. Andersson, E. Förster, K. Witte, *Phys. Rev. Lett.* **82**, 4843 (1999).
- ⁵ N. C. Woolsey, C. A. Back, R. W. Lee, A. Calisti, C. Mossé, R. Stamm, B. Talin, A. Asfaw, L. S. Klein, *J. Quant. Spectrosc. Radiat. Transfer* **65**, 573 (2000).
- ⁶ H. Nguyen, M. Koenig, D. Benredjem, M. Caby, and G. Coulaud, *Phys. Rev. A* **33**, 1279 (1986).
- ⁷ D. Kalantar, et al., in *Proceedings from the SPIE 1996 Congress on High-Speed Photography and Photonics* (1997).
- ⁸ G. C. Junkel, M. A. Gunderson, D. A. Haynes, Jr., and C. F. Hooper, Jr., “Full-Coulomb calculation of Stark broadened spectra from multi-electron ions: A focus on the dense plasma line shift”, submitted to *Phys. Rev. E* (2000).
- ⁹ M. A. Gunderson, G. C. Junkel, D. A. Haynes, Jr., and C. F. Hooper, Jr., *Bull. Amer. Phys. Soc.* **44**, 178 (1999).
- ¹⁰ H. R. Griem, *Principles of Plasma Spectroscopy* (Cambridge University Press, Cambridge, 1997).
- ¹¹ C. A. Iglesias, J. L. Lebowitz, and D. A. MacGowan, *Phys. Rev. A* **28**, 1667 (1983).
- ¹² D. B. Boercker, C. A. Iglesias, and J. W. Dufty, *Phys. Rev. A* **36**, 2254 (1987).
- ¹³ D. A. Haynes, Jr., D. T. Garber, C. F. Hooper, Jr., R. C. Mancini, Y. T. Lee, D. K. Bradley, J. Delettrez, R. Epstein, and P. A. Jaanimagi, *Phys. Rev. E* **53**, 1042 (1996).
- ¹⁴ J. Cooper, D. E. Kelleher, and R. W. Lee, in *Proceedings of the 2nd International Conference on the Properties of Hot Dense Matter* (World Scientific Press, Singapore, 1985).
- ¹⁵ H. R. Griem, M. Blaha, and P. C. Kepple, *Phys. Rev. A* **41**, 5600 (1990).
- ¹⁶ Inglis and Teller, *Astrophys. J.* **90** (1939).
- ¹⁷ D. G. Hummer and D. Mihalas, *Ap. J.* **331**, 794 (1988).